

1 Generating samples of extreme 2 winters to support climate adaptation

3 **Nicholas J. Leach^{1*}, Peter A. G. Watson², Sarah N. Sparrow³, David C. H. Wallom³,**
4 **David M. H. Sexton⁴**

5 ¹ Atmospheric, Oceanic, and Planetary Physics, Department of Physics, University of Oxford,
6 Oxford, UK

7 ² School of Geographical Sciences, University of Bristol, Bristol, UK

8 ³ Oxford e-Research Centre, Engineering Science, University of Oxford, Oxford, UK

9 ⁴ Met Office Hadley Centre, Exeter, UK

10 • Corresponding author. *Email:* nicholas.leach@stx.ox.ac.uk

11 Key Points

- 12 • We create 3x1000-member ensembles in an atmosphere-only model, taking
13 boundary conditions from coupled simulations of future extreme winters
- 14 • The boundary conditions in two of the three winters favour extreme winters and we
15 find examples that are beyond 1-in-10000 year events
- 16 • These high-end extremes could be used for more robust adaptation planning and
17 climate scenario development

18 Abstract

19 Recent extreme weather in the UK highlights the need to understand the potential for more
20 extreme events in the present-day, and how such events may change with global warming. We

21 present a methodology for more efficiently sampling extremes in future climate projections.
22 As a proof-of-concept, we use the UK's most recent set of national Climate Projections
23 (UKCP18). UKCP18 includes a 15-member perturbed parameter ensemble (PPE) of coupled
24 global simulations, providing a range of climate projections incorporating uncertainty in both
25 internal variability and forced response. However, this ensemble is too small to adequately
26 sample extremes with return periods over 100 years, which are of interest to policy-makers
27 and adaptation planners. To better understand the statistics of these events, we use
28 distributed computing to run three ~1000-member initial-condition ensembles with the
29 atmosphere-only HadAM4 model at 60km resolution on volunteers' computers, taking
30 boundary conditions from future extreme winters within the UKCP18 ensemble. We find that
31 every UKCP18 extreme winter is captured within our ensembles, and that two of the three
32 ensembles are conditioned towards producing extremes by the boundary conditions. Our
33 ensembles contain several extremes that would only be expected to be sampled by a UKCP18
34 PPE of over 500 members, which would be prohibitively expensive with current
35 supercomputing resource. The most extreme winters simulated lie above those for UKCP18
36 by 0.85K for daily maximum temperature and 37% of the present-day average for
37 precipitation (UK winter means).

38 Plain language summary

39 The risk from extreme weather events is important to understand due to the damage that
40 they can cause. This study is concerned with understanding extremes both in the
41 present-day, and how they may change with global warming. Extreme weather events can be
42 difficult to study with climate models due to their rarity: sampling the most extreme events
43 requires very long simulations. In a climate model containing a representation of both the
44 atmosphere and ocean such long simulations would be prohibitively expensive. In this study

45 we explore a new approach for efficiently sampling extremes over the UK (though it is
46 applicable to other regions). Starting with a small sample of coupled climate model
47 simulations, we use surface temperature and sea ice conditions from the most extreme
48 future winters within these coupled simulations to drive an atmosphere-only model. We run
49 this model on volunteers' personal computers, which allows us to create very large
50 ensembles of simulated winter weather. Our ensembles contain many samples of very
51 extreme events; some sea surface temperature patterns condition the ensemble towards
52 producing extremes. Our approach could be used to explore the uncertainty surrounding
53 extreme weather events at the present-day, or create climate scenarios to inform adaptation
54 planning.

55 Key words

56 climate modelling | climate change projection | understanding extreme weather events | large
57 ensembles | climate change adaptation

58 1. Introduction

59 Weather extremes are one of the most damaging hazards that society faces at the
60 present-day (*The Global Risks Report 2021*, 2021). Many studies have now found that
61 anthropogenic climate change is increasing the frequency and/or magnitude of certain types
62 of extreme weather, including heatwaves, extreme rainfall and droughts (Seneviratne et al.,
63 2021). This has therefore resulted in a need to plan how society can adapt to the more
64 frequent or severe weather extremes projected to occur under continued greenhouse gas
65 emissions (M. R. Allen et al., 2009; Diffenbaugh et al., 2017; Rahmstorf & Coumou, 2011). In

66 order to plan effectively, we must first understand and quantify how extreme weather events
67 are projected to change into the future.

68 In the United Kingdom (UK), a key part of this understanding has been informed by the UK
69 Climate Projections (UKCP) project. The most recent iteration of UKCP (UKCP18) was
70 released in 2018 (Lowe et al., 2018; Murphy et al., 2018) and included a number of novel
71 climate model ensembles: a set of transient global simulations from coupled climate models,
72 with 15 simulations from a single-model perturbed parameter ensemble (PPE) and 13
73 additional simulations from CMIP5 models; a set of 12 regional climate model simulations;
74 and a set of 12 convection permitting model projections. In this study, we focus on the set of
75 15 PPE simulations, and our analysis and results build upon the information provided by
76 these global runs.

77 In particular, we are interested in how effectively the UKCP18 PPE has sampled extreme
78 weather during the UK winter, and in exploring methods for improving the sampling of
79 extremes that could inform the design of future projections. To this end, we aim to provide
80 proof-of-concept of a methodology for generating large ensembles of extreme winters. We
81 first select three exceptional UK winters from the UKCP18 PPE that occurred between 2061
82 and 2080 (henceforth the “study winters”). We then use the sea surface temperature (SST)
83 and sea ice (SIC) fields from these winters to force very large perturbed initial-condition
84 ensembles using the HadAM4 model, which has been implemented to run in the distributed
85 computing system *climateprediction.net* at the same horizontal resolution as the UKCP18
86 global simulations. This allows very large ensembles to be produced and is possible because
87 HadAM4 requires less computational resources. These ensembles are intended to provide
88 numerous extreme samples, hence are called the “ExSamples” ensembles. We compare the
89 statistics of weather extremes in these ExSamples ensembles to both the corresponding

90 extreme study winter, and to the whole UKCP18 PPE 2061-2080 climate distribution in order
91 to answer several science questions:

- 92 ● Is the atmosphere-only model able to produce equal magnitude extremes to those
93 within the study winters from the UKCP18 PPE? If the study winter lies outside the
94 atmosphere-only model distribution, this suggests the importance of coupling to a
95 dynamic ocean and other differences between the models for producing extremes.
- 96 ● Were the study winters truly exceptional, or could they have been even more extreme?
- 97 ● To what extent did the SSTs and SIC during the study winters condition the extreme
98 response?
- 99 ● Is carrying out this type of experiment using a computationally cheaper, but less
100 modern, atmosphere-only model a better methodology for sampling extremes than
101 increasing the size of the UKCP18 PPE?

102 In this paper, we first describe the models used, experiment design and statistical
103 methodologies performed within the study. We then present the results of our experiments,
104 first comparing the climate distributions of the two models over a present-day baseline
105 period to assess whether there are any significant biases between them. Taking any biases
106 into account, we compare the projections from our three future ensembles to the UKCP18
107 PPE, focussing on how the extreme tail of the climate distribution is sampled. This
108 comparison allows us to explore the sampling advantage given by, and influence of, the SST
109 and SIC. The very large ensembles created also allow us to examine the influence of the
110 large scale dynamics present during the study winters using a circulation analog approach.
111 We then use a single ensemble member case study to highlight the importance of large
112 ensembles for sampling unprecedented extreme events that cannot always be statistically
113 extrapolated from smaller ensembles (Fischer et al., 2021; Gessner et al., 2021). Finally, we

114 discuss the insights provided by these experiments, and how they might inform the design of
115 future projections; also suggesting directions for future research that could further improve
116 our approach.

117 **2. Study design and methods**

118 **2.1 Models**

119 **2.1.1 HadGEM3-GC3.05 global climate model**

120 In addition to the ExSamples ensembles, we also analyse UKCP18 global PPE simulations of
121 the RCP8.5 emission scenario (Riahi et al., 2011). This PPE is based on the global
122 HadGEM3-GC3.05 coupled ocean atmosphere model (Murphy et al., 2018; Williams et al.,
123 2018). This combines an 85 vertical level atmosphere model at 5/6 ° zonal and 5/9 °
124 meridional resolution (N216, ~60 km at mid-latitudes) with a 75 level ocean model at
125 ORCA025 (1/4 °) horizontal resolution. The aim of this PPE is to explore a range of plausible
126 model responses to climate change. The parameters were selected on the basis of the
127 credibility of the model response on both weather and climate timescales (Karmalkar et al.,
128 2019; D. M. H. Sexton et al., 2019, 2021; Yamazaki et al., 2021). In this study we use both the
129 final product 15-member PPE and a 10-member subsample. The 10-member subsample
130 consists of the 12 members that compose the accompanying UKCP18 regional climate model
131 projections (Murphy et al., 2018), minus two members that displayed a significant weakening
132 of the Atlantic Meridional Overturning Circulation (D. Sexton et al., 2020). Henceforth, we
133 shall refer to the HadGEM3-GC3.05 simulations analysed here as the “UKCP18 PPE”. Unless
134 stated otherwise, this refers to the 15-member PPE.

135 2.1.2 HadAM4 N216 atmospheric model

136 The novel simulations presented here are performed by the global HadAM4 atmosphere and
137 land surface model (Webb et al., 2001; Williams et al., 2003). Like its predecessor, HadAM3
138 (Pope et al., 2000), it includes prognostic cloud, convection and gravity-wave drag
139 parameterisation schemes, a radiation scheme that treats water vapour and ice crystals
140 separately, and a land surface scheme. The updates in HadAM4 include a mixed-phase
141 precipitation scheme, parameterisation of ice cloud particle size and the radiative effects of
142 non-spherical ice particles, and a revised boundary layer scheme. The version used here
143 incorporates an upgrade to the spatial resolution (Bevacqua et al., 2021; Watson et al., 2020),
144 which matches the horizontal resolution of the HadGEM3-GC3.05 simulations analysed here.
145 HadAM4 has 38 vertical levels; and here the sea surface temperature (SST) and sea ice
146 fraction (SIC) boundary conditions are taken from specific years and members of the
147 HadGEM3-GC3.05 UKCP18 PPE simulations.

148 A key aspect of the HadAM4 simulations described here are that they are performed on the
149 personal computers of volunteers using the *climateprediction.net* distributed computing
150 system (M. Allen, 1999; Anderson, 2004; D. Stainforth et al., 2002). This system has been
151 used previously to run a range of Hadley Center Unified Model variants (A. Brown et al., 2012),
152 including a coupled atmosphere-slab ocean model (D. A. Stainforth et al., 2005), a fully
153 coupled model (Frame et al., 2009) and an atmosphere-only model (Pall et al., 2011) similar
154 to HadAM4. The near thousand member ensembles presented here would be prohibitively
155 expensive to run using a standard supercomputer, and so we are only able to run the
156 bespoke experiments presented in this study because of this distributed computing system,
157 and the volunteers involved. However, the constraints of this system strongly motivate the
158 choice of HadAM4: it is sufficiently memory-efficient that it can be run on personal

159 computers at the same horizontal resolution as the state-of-the-art HadGEM3-GC3.05
160 model.

161 Henceforth, we shall refer to the HadAM4 simulations presented here as the “ExSamples”
162 ensembles. A complete description of the ExSamples ensembles, including the selection of
163 the prescribed SST/SIC, is given below in “Experiment design”.

164 2.2 ExSamples experiment design

165 ExSamples covers six distinct sets of simulations: three future winter and three baseline
166 period ensembles. The process behind generating each future and corresponding baseline
167 ensemble is as follows:

- 168 1. Select a single winter from within the UKCP18 PPE over the 2061-2080 period. This
169 winter is chosen on the basis of being particularly “extreme”; more detail on how we
170 selected the three future winters is given below in [“Selecting the three “extreme”
171 study winters”](#).
- 172 2. Use the SSTs and SICs from this winter to force HadAM4 over the November - March
173 period (the November of each simulation is used to spin-up the simulation and is
174 discarded prior to analysis). An ensemble is created from the boundary conditions for
175 this single winter through initial-condition perturbations. Due to the nature of the
176 (ongoing) distributed computing system used to run the model (M. Allen, 1999; D. A.
177 Stainforth et al., 2005), our target final ensemble size is 1500 members, and in this
178 study we analyse all the members that are complete at the time of writing and pass
179 our quality control checks, which ranges from 883 to 1036 over the three ensembles
180 (Sparrow et al., 2021).

181 3. We then create a corresponding HadAM4 baseline ensemble by using winter SSTs
182 and SICs from the same UKCP18 member as the selected winter over the period
183 2007-2016. For each of the ten years, an ensemble of 50 members is generated
184 using initial-condition perturbations. This results in a target baseline ensemble size
185 of 500 members per study winter.

186 2.2.1 Motivation of the experiment design

187 In this section we outline the motivation behind our experimental design, with a particular
188 focus on the differences between the internal variability sampled by a coupled model, and
189 sampled by an atmosphere-only model. The coupled PPE in UKCP18 samples a series of
190 events including the most extreme ones, that arise from the response to anthropogenic
191 forcing plus coupled internal variability. The latter is due to a combination of internal
192 variability in the ocean, the impact this has on the atmosphere, and internal variability
193 generated within the atmosphere itself (Sexton et al., 2001). So an extreme deviation about
194 the long-term forced trend in a coupled simulation might have occurred solely due to
195 atmospheric internal variability but it is a priori more likely than other years to have had a
196 contribution from ocean internal variability. Therefore, by picking three winters with the
197 largest deviations from the long-term climate trend, we hope to capture more winters where
198 the ocean has strongly influenced the extreme. In years where there is an appreciable
199 influence from ocean internal variability, which will be manifest in the simulated SST and SIC
200 patterns along with the long term forced response of the ocean to anthropogenic forcing,
201 then there is more potential for there to be an additional effect from atmospheric internal
202 variability to produce greater extremes. Therefore an initial-condition ensemble of
203 atmosphere-only simulations forced by SSTs, SIC and anthropogenic forcing from a study
204 winter, where members differ only by atmospheric internal variability, can be used to
205 distinguish winters where the ocean internal variability has played an important role from

206 ones where the ocean has played little role. In the former case, we would expect to sample
207 extremes beyond the UKCP18 extreme more often than we would by chance from
208 atmospheric internal variability around the long term forced response.

209 2.2.2 Definitions of key terms

210 There are several technical definitions we use throughout this study, which we will define in
211 this section.

212 Firstly, a “raw value” is the simulated value straight from the model, as found within the
213 relevant data product.

214 “Anomalies” are these raw values set relative to the average absolute value over some
215 reference period, in order to remove any mean model biases. For the ExSamples simulations,
216 we define anomalies as the raw values minus the average over the corresponding 2007-2016
217 baseline ensemble members. For the UKCP simulations, we define anomalies as the raw
218 values minus the 1997-2026 reference period mean for each PPE member. This longer
219 30-year period is used to reduce the impact of inter-decadal variability that may be present
220 in the time series of each member. For precipitation, we show results in terms of the
221 “percent change” to compensate for differences in average rainfall intensity between the two
222 models used. Percent changes are calculated as anomalies divided by the average raw value
223 over the reference period (times 100 %).

224 Finally, we use “deviations” in the context of the UKCP PPE to refer to the raw values relative
225 to a long-term trend. Deviations are calculated as the residual of a simple linear regression
226 computed over time for each PPE member (ie. over the 2061-2080 period). Deviations
227 therefore represent a basic estimate of the variability about a long-term forced trend. Hence
228 we use deviations to measure how unusual a particular simulated winter within the UKCP18
229 PPE is compared to others when a forced trend that may vary across ensemble members is

230 present; and also to generate time series that can be fitted using statistical models that
231 assume the underlying process is stationary. Deviations of the UKCP18 PPE also provide the
232 closest simple comparison to the atmosphere-only ExSamples ensembles which only sample
233 atmospheric internal variability.

234 2.2.3 Selecting the three “extreme” study winters

235 To generate our future ExSamples ensembles, we needed to select three “extreme” winters
236 from the UKCP18 PPE projections. We considered winters from the 10-member subsample
237 over the period 2061-2080, giving a total of 200 candidate winters for selection. The
238 10-member subsample was used such that the ExSamples ensembles generated here would
239 be able to be directly compared to the UKCP18 regional climate and convection permitting
240 model projections if desired in the future.

241 The variables we used to compare how “extreme” each candidate winter was were the winter
242 (DJF) mean of daily maximum temperatures, and winter mean precipitation, each averaged
243 over the UK land region. Since the UKCP18 PPE displays significant forced trends in climate
244 over the 2061-2080 period and based on the thinking behind the experimental design, we
245 used the deviations of each candidate winter as the basis for our selection; if we used
246 anomalies we would naturally bias our selection towards the end of the period.

247 We aimed to select two “hot” winters and one “wet” winter. As shown in Figure 1, there is one
248 clear candidate for each type of extreme: UKCP18 PPE member 02868 (ID numbers as
249 Sexton et al., 2021) year 2066 as a hot winter; and member 02242 year 2068 for the wet
250 winter. The next most extreme hot winters shown in Figure 1A all had similar deviations, so
251 we distinguished between them on the basis of their anomalies, choosing member 01554
252 year 2072, which has the highest anomaly of any of the candidate winters.

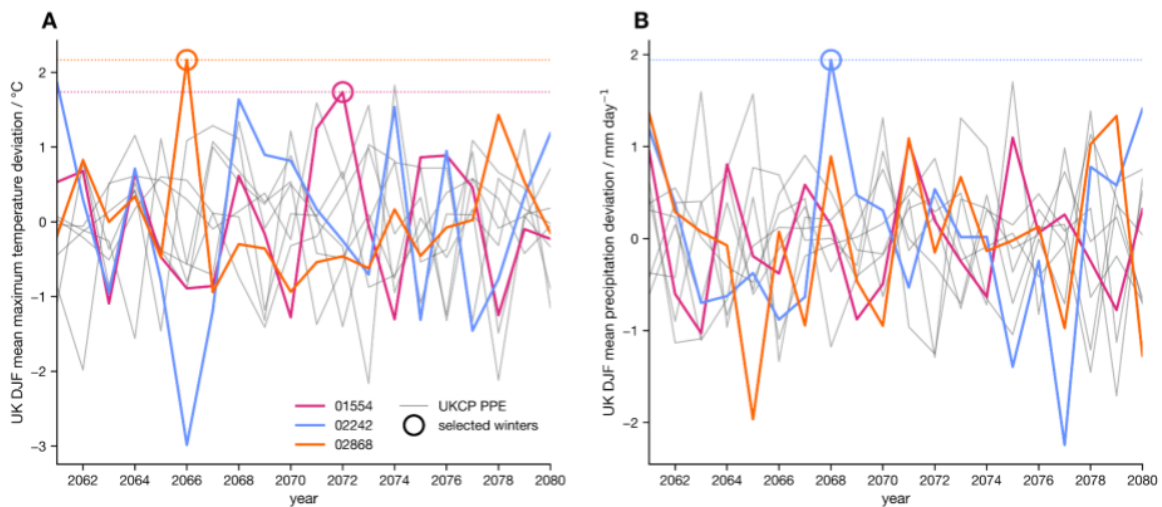


FIG 1: UKCP PPE 2061-2080 deviations. **A**, DJF mean of daily maximum temperatures averaged over the UK region. Coloured lines indicate the three UKCP runs from which the study winters were chosen. The study winters are circled and dotted horizontal lines indicate the deviation of each study winter. The ensemble member id of the three runs is given in the legend. **B**, as **A**, but for DJF mean precipitation.

253 Table 1 provides a summary of the study winters selected. For clarity, we refer to the
 254 ExSamples ensembles by the abbreviations given in the final column of Table 1 followed by “
 255 ensemble” (so the ensemble that uses the SST/SIC from UKCP18 member 02868 year 2066
 256 is “HOT1 ensemble”, and the corresponding baseline ensemble is “HOT1-B ensemble”). We
 257 use “aggregate baseline ensemble” to denote the aggregate of all three baseline ensembles.
 258 We refer to the corresponding winters as the ensemble abbreviation followed by “winter”.
 259 Finally, we refer to the UKCP18 PPE ensembles as “UKCP” followed by the period the samples
 260 are taken from.

	Boundary condition (study winter) info			Abbreviation used
	UKCP18 member	Year	Extreme type	
Future projections	02868	2066	HOT	HOT1
	01554	2072	HOT	HOT2
	02242	2068	WET	WET1
Baseline ensembles	02868	2007-2016	-	HOT1-B
	01554	2007-2016	-	HOT2-B
	02242	2007-2016	-	WET1-B

Table 1: Summary of experiments performed for ExSamples project.

261 2.2.4 Synoptic characterisation of the study winters

262 Here, we briefly describe the broad synoptic characteristics of each of the three future
263 winters selected. Figure 2 shows three key characteristics: mean sea level pressure (MSLP)
264 anomalies over the UK; SST deviations; and Arctic SICs. They display a wide range of
265 meteorological and climatological features: none of the extreme winters selected are caused
266 by very similar large-scale features.

267 The HOT1 winter displays a strong positive NAO pattern. Over the UK the flow is even more
268 zonal, and has a weaker gradient; the positive NAO pattern is also weaker. This shares
269 similarities with several weather patterns, including 20 and 23. There is a strong positive
270 ENSO phase during this winter, alongside moderately positive Atlantic Multidecadal
271 Variability and negative phase Pacific Decadal Oscillation. This extreme winter places
272 between the other two in terms of SIC - mean Arctic sea ice fraction is approximately 70 %.

273 The HOT2 winter displays a similar MSLP pattern to the first hot winter. In terms of the 30
274 weather patterns developed by the Met Office (Neal et al., 2016), the mean large scale flow
275 over the whole winter is closest to weather pattern 20. This weather pattern is associated
276 with warm and wet weather over the UK (Huang et al., 2020; Richardson et al., 2018, 2020),
277 and has also been shown to be conducive to producing record temperature extremes on daily
278 timescales (Kendon et al., 2020). During this winter, the El Nino Southern Oscillation (ENSO)
279 pattern of global SST variability was in a weak La Nina (negative) phase (Deser et al., 2010);
280 this phase has previously been linked to an increased likelihood of positive NAO (Deser et al.,
281 2017; M. P. King et al., 2018, 2020; López-Parages et al., 2016). No other modes of SST
282 variability are present. With regards to SIC, this particular PPE member has virtually entirely
283 lost all winter Arctic sea ice by 2072. It has been suggested that Arctic sea ice loss may be
284 linked with more persistent mid-latitude weather patterns (Francis & Vavrus, 2012; Pedersen
285 et al., 2016), though this is still a subject of active scientific interest (Kretschmer et al., 2020;
286 Screen, 2017; Screen & Simmonds, 2013).

287 The WET winter displays a strong cyclonic south westerly flow with a low west of Ireland;
288 classified as weather pattern 29. This pattern is associated with generally warm and wet
289 weather. ENSO is in a neutral phase during this winter; and there are no other modes of SST
290 variability in significantly positive or negative phases. Of the three study winters, this one has
291 the smallest change in sea ice relative to the present-day; Arctic sea ice is almost entirely
292 intact over the winter.

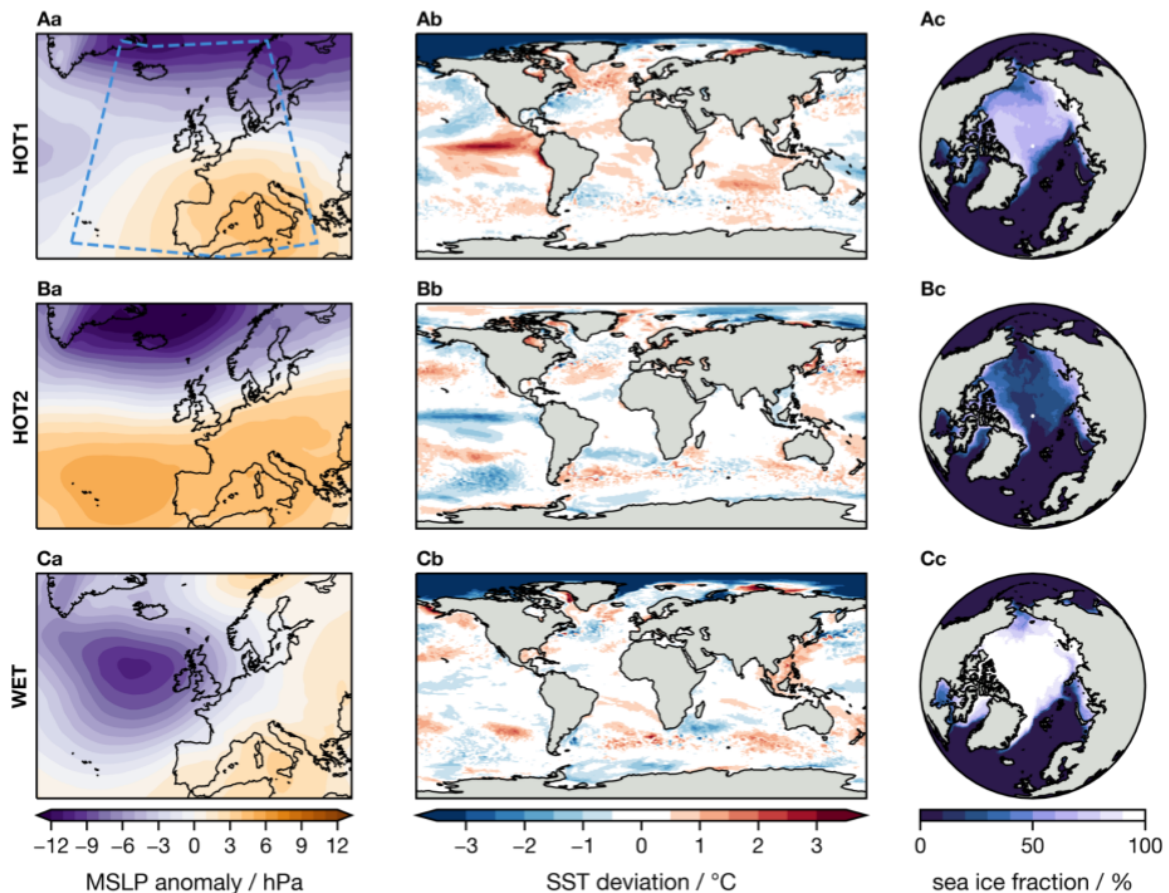


FIG 2: synoptic features of the study winters within the UKCP simulations. The row titles indicate the study winter. **a**, DJF mean MSLP anomalies for each winter. **b**, DJF mean SST deviations for each winter. Deviations are calculated for each gridpoint timeseries over 2061-2080. **c**, DJF mean Arctic sea ice fraction for each winter. The blue dashed line in Aa indicates the area used for analog subsampling.

293 2.3 Statistical methods

294 2.3.1 Estimating distributions of extremes

295 We estimate distributions using the method of L-moments (Hosking, 1990; Hosking et al.,

296 1985; Hosking & Wallis, 1997). We use L-moments for their computational efficiency and

297 stability. Uncertainties in the fit distributions, their CDFs and corresponding return periods

298 are calculated using a 10,000 resample nonparametric bootstrap. The specific distributions

299 used for each variable analysed are as follows:

300 Mean DJF daily maximum temperatures (TXm) & daily mean precipitation rate (PRm)

301 We use a generalised pareto distribution (Coles, 2001; Hosking & Wallis, 1987) fit to the
302 upper quantile of the sample population. When estimating CDFs and corresponding return
303 periods from the fit, if the value in question lies below the upper quantile, we use the
304 empirical CDF.

305 Maximum DJF daily maximum temperatures (TXx)

306 We use a generalised extreme value distribution fit to the sample population.

307 Maximum DJF daily mean precipitation rate (PRx)

308 We use a generalised logistic distribution (Hosking, 1990) fit to the sample population. A
309 generalised logistic distribution is used since the tail of the UKCP18 PPE 2061-2080
310 deviations population is clearly heavier than estimated by best-fit generalised extreme or
311 generalised pareto distributions; we note that this approach to modelling block maxima of
312 daily rainfall has some precedent in the literature (Kysely & Picek, 2007; Wan Zin et al.,
313 2009). This issue is not a feature of the L-Moments estimator used: a maximum likelihood
314 estimator yields near-identical results. The apparent discrepancy with the generalised
315 extreme value distribution may arise as the number of independent precipitation events per
316 season may not be near enough to the asymptotic limit (independent event count $\rightarrow \infty$) for
317 classical extreme value theory to be appropriate, as noted previously for annual daily rainfall
318 maxima (Marani & Ignaccolo, 2015).

319 2.3.2 Analog construction

320 In order to assess the dynamical contributions to the extreme weather simulated during the
321 study winters, we use an MSLP analog approach (Cattiaux et al., 2010; Vautard et al., 2016;
322 Yiou et al., 2017). For each future ExSamples ensemble (and each corresponding baseline

323 ensemble), we create a subsample of analogs composed of ensemble members that have a
324 root mean square error (Euclidean distance) of less than 3 hPa from the UKCP18 PPE study
325 winter average MSLP over the domain enclosed by the dashed blue lines in the top left
326 subplot of Figure 2 (-30:20°E; 35:70°N). This domain was the best for explaining variance in
327 UK temperatures and close to best for UK precipitation of those investigated by (Neal et al.,
328 2016). We used a 3hPa threshold as this was the tightest constraint that resulted in analog
329 ensembles large enough to infer statistics from with any degree of certainty (>20 members
330 in each case). The MSLP distance based subsampling results in an ensemble of analogs in
331 which the mean large scale flow during the winter very closely matches the study winter. We
332 can then use these ensembles of analogs to estimate the dynamical contribution and
333 associated uncertainty to the extreme weather.

334 **3. Results**

335 **3.1 Comparison of HadAM4 and HadGEM3-GC3.05 baseline** 336 **ensembles**

337 Before we can robustly compare the projections within the UKCP18 PPE and ExSamples
338 ensembles, we must first quantify any differences between the representations of UK climate
339 within the HadAM4 and HadGEM3-GC3.05 models. We do this by comparing the 15-member
340 UKCP18 PPE over 2007-2016 (150 members total) with each of the three 2007-2016
341 ExSamples baseline ensembles (~500 members each) in turn, and their aggregate ensemble.
342 Here we quantify whether the simulated climates differ using a two-sample
343 Kolmogorov-Smirnoff (K-S) test (Hodges, 1958; Kolmogorov, 1933; Smirnoff, 1939a, 1939b) at
344 the 5 % significance level on the anomalies of the variable in question unless stated

345 otherwise. We use anomalies here since our main results are presented using anomalies to
346 account for any model mean biases (and biases between different UKCP18 PPE members),
347 but note if there are significant differences between the two model climate means. Verifying
348 the accuracy of these models against reality lies outside of the scope of this paper, but has
349 already been studied for both the UKCP18 PPE (Murphy et al., 2018) and HadAM4 (Bevacqua
350 et al., 2021; Watson et al., 2020).

351 For both mean and maximum DJF daily maximum temperatures over the UK (TXm and TXx
352 respectively), the UKCP 2007-2016 and ExSamples baseline distributions are highly
353 comparable (Figures 3, 4, S4, S7, S8, S9). None of the three (nor their aggregate) ExSamples
354 baseline ensemble distributions are statistically significantly different from the
355 corresponding UKCP baseline ensemble distributions for either TXm or TXx anomalies. The
356 ExSamples aggregate baseline ensemble mean biases are +0.06 K and +0.18 K compared to
357 the UKCP18 PPE for TXm and TXx respectively.

358 For mean DJF precipitation rate over the UK (PRm), we do find clear differences in the
359 behaviour of the models. The ExSamples baseline ensembles have a reduced winter average
360 rainfall intensity compared to the UKCP18 PPE: a 16 % (0.61 mm day^{-1}) lower ensemble mean.
361 They also have a slightly increased spread in winter rainfall. We note that these differences in
362 simulated UK climate do not appear to be the result of differences in the large-scale
363 dynamics of the two models over the Euro-Atlantic sector; as investigated using a Principal
364 Component Analysis in the [Supplementary Information](#). Despite the difference in spread,
365 none of three ExSamples baseline ensemble distributions are statistically significantly
366 different from the UKCP18 baseline ensemble distribution for absolute PRm anomalies; nor is
367 their aggregate. However, due to this discrepancy in mean rainfall intensity between the two
368 models, we measure projected PRm in percent changes rather than anomalies, both in the
369 figures presented and analysis carried out. After converting to percentages, the differences

370 in the spread of the distributions becomes relatively larger (Figure 5) and the distributions of
371 percentage anomalies are statistically significantly different.

372 Despite the differences in PR_m, the two models show little difference in their simulated
373 distributions of the DJF maximum of daily mean precipitation averaged over the UK (PR_x).

374 The difference in mean PR_x between all the ExSamples baseline ensembles and the UKCP18
375 PPE is only 4 % (0.99 mm day⁻¹). None of the three (nor their aggregate) ExSamples baseline
376 ensembles are statistically significantly different from the UKCP 2007-2016 distribution for
377 PR_x anomalies.

378 3.2 Projections of future extremes

379 In this section we examine the future ExSamples ensembles and compare them to the
380 UKCP18 PPE projections. Since we are largely concerned with winters that are extreme as a
381 whole, rather than isolated extreme weather events within the winters (consistent with our
382 methodology for selecting the three study winters), we analyse “hot” winters through
383 DJF-mean temperatures and “wet” winters through DJF-mean precipitation.

384 3.2.1 HOT1

385 We first address the primary question: was the atmosphere-only HadAM4 model able to
386 capture the magnitude of the extreme simulated in the study winter by the coupled
387 HadGEM3-GC3.05 model? Yes - there are four within the HOT1 ensemble that exceed the
388 TX_m value of the study winter, as shown in Figure 3.

389 However, the prescribed SST/SIC within the HOT1 simulations do not appear to have
390 conditioned this ensemble towards producing more extremes than would be expected from
391 an (unconditioned by construction) UKCP18 PPE of the same (increased) size. This is clearly
392 seen in Figure 3: the distributions of the HOT1 and UKCP 2061-2080 ensembles are very

393 similar in the PDF subplot; and the ExSamples return period sample histogram follows the
394 “1000 member” expectation line closely. We can conclude that despite the HOT1 winter
395 being an exceptional extreme within the context of the UKCP18 PPE, the associated SST and
396 SICs did not pre-condition the winter towards (nor away from) such an extreme.

397 In order to compare the conditioning (effectively the “sampling advantage”) across the three
398 ensembles, we examine the relative exceedance risk of three different extreme thresholds set
399 by the following UKCP18 PPE distribution quantiles: 0.9, 0.95 and 0.99; representing 1-in-10,
400 -20 and -100 year extremes. We do this for both the TXm and PRm variables. We first
401 calculate the threshold values that correspond to the given extremes using the UKCP
402 2061-2080 deviations statistical fit (ie. the black line in Figure 3B). We then calculate the
403 fractions of the UKCP 2061-2080 and ExSamples ensembles that lie above these thresholds.
404 We present the results in Table 2 in terms of the relative risk of the given extreme in the
405 ExSamples ensemble compared to the UKCP ensemble. This is calculated as the fraction of
406 the ExSamples ensemble that exceeds the threshold divided by the corresponding fraction of
407 the UKCP ensemble, analogous to the “risk ratios” often used in extreme event attribution
408 studies (Stone & Allen, 2005; Stott et al., 2004). This relative risk provides a measure of how
409 many more samples of extremes of a particular return period we would expect to see in the
410 ExSamples ensembles compared to a UKCP18 PPE-style ensemble of equal size. The
411 quantitative results in Table 2 support the picture provided by Figure 3: the HOT1 ensemble
412 was not conditioned towards producing any more extremes than expected from the
413 unconditioned UKCP 2061-2080 ensemble (for several thresholds it actually appears to have
414 been marginally conditioned away from producing extremes).

415 While the boundary conditions did not have any impact on the likelihood of an extreme
416 winter, the large-scale dynamical situation of the study winter did. According to the analogs
417 within the HOT1 ensemble, this specific dynamical situation increased the chance of a

418 1-in-100 year winter (based on the UKCP 2061-2080 statistical fit in Figure 3B) by a factor of
419 6.2 [5.3 , 6.9]. A similar level of dynamical conditioning is seen in the baseline ensemble. The
420 analog-based subsampling also suggests that the prescribed SST/SIC may actually make the
421 dynamical situation of the study winter less likely to occur than expected from the baseline
422 climatological rate: the proportion of analogs in the HOT1 ensemble is 20 % lower than in
423 the HOT1-B ensemble. Note that this change in analog frequency is not significant at the 5 %
424 level. This change is reflected in the HOT1 ensemble mean MSLP anomalies, which are
425 negative southwest of the UK and positive northwest of the UK (the opposite pattern to the
426 study winter).

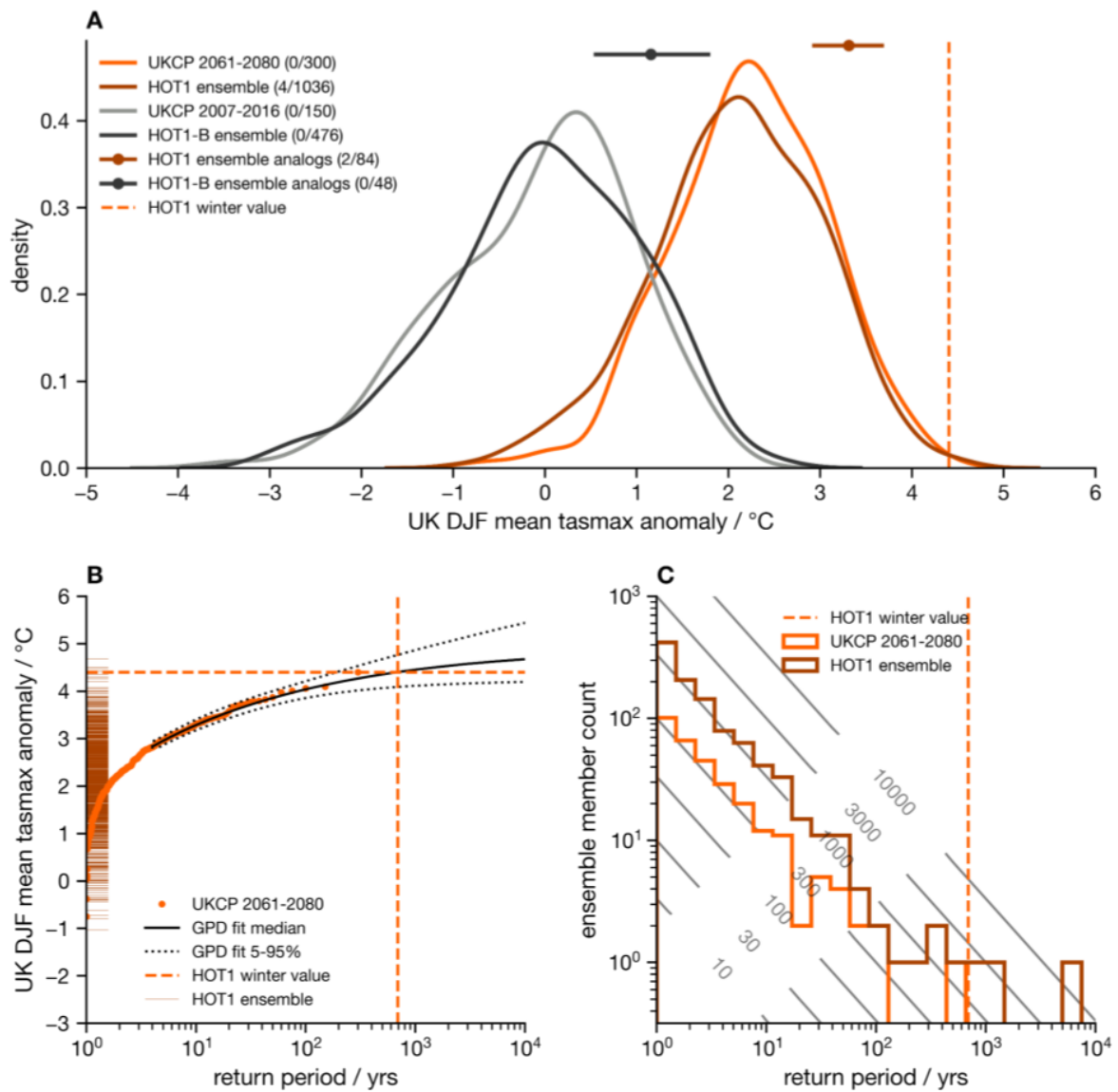


FIG 3: comparing statistics of DJF mean of daily maximum temperatures averaged over the UK region for the HOT1 winter. **A**, PDFs of baseline and future ensembles. The light orange PDF shows UKCP 2061-2080 deviations, with the distribution mean set to the ensemble mean anomaly between 2007-2016 and 2061-2071. The dark orange PDF shows HOT1 ensemble anomalies. The light grey PDF shows UKCP 2007-2016 anomalies. The dashed horizontal light orange line indicates HOT1 winter deviation. The dark orange and black dotted bars indicate mean and likely range (16-84 %) of corresponding analog subsamples. The bracketed values in the legend indicate the number of ensemble members that exceed the HOT1 winter threshold over the total number of ensemble members. **B**, return period diagram. The light orange dots show the empirical CDF of UKCP PPE 2061-2080 deviations. The solid black line shows the median generalised pareto distribution fit. The dotted black lines indicate a 5-95 % credible interval of the distribution fit. The dark orange dashes along left y axis indicate positions of HOT1 ensemble anomalies. **C**, histograms of sampled return periods. The light orange line indicates the UKCP 2061-2080 deviations histogram, and the dark orange line the HOT1 ensemble anomalies. The dashed light orange line indicates the best-estimate return period of the HOT1 winter deviation. Black contours indicate the expected histogram curve arising from a sample of size given by the contour labels.

We note that the sampled return periods are calculated using the best-estimate fit distribution shown in the return period diagram; hence the curves in **C** and **A** are related by the transfer function indicated by the solid black line in **B**.

Study winter	Variable	UKCP18 quantile (return period)		
		0.9 (1-in-10 year)	0.95 (1-in-20)	0.99 (1-in-100)
HOT1	TXm	0.9 [0.86 , 0.96]	0.84 [0.77 , 0.97]	0.97 [0.75 , 2.32]
	PRm	1.02 [0.95 , 1.08]	0.98 [0.85 , 1.03]	2.03 [1.0 , 3.78]
HOT2	TXm	4.25 [3.95 , 4.64]	5.71 [4.97 , 6.05]	9.97 [7.34 , 24.8]
	PRm	2.93 [2.5 , 3.22]	3.6 [3.17 , 3.81]	10.08 [4.5 , 16.19]
WET1	TXm	3.75 [3.61 , 4.06]	4.3 [3.67 , 4.7]	5.02 [3.53 , 10.14]
	PRm	3.96 [3.42 , 4.22]	4.7 [4.22 , 4.94]	11.75 [6.17 , 17.14]

Table 2: Relative risk of three extreme thresholds in ExSamples future ensembles compared to UKCP18 PPE 2061-2080 deviations. Square brackets indicate a 90 % CI.

427 3.2.2 HOT2

428 Again, the magnitude of the extreme in the study winter was captured within the HOT2

429 ensemble.

430 The HOT2 ensemble produced more extremes than would be expected from a UKCP18 PPE

431 ensemble of the same size (Figure 4A, C, Table 2), suggesting that it was preconditioned

432 towards such extremes by the prescribed SST/SIC. We can see from Figure 4C that the HOT2

433 ensemble samples extremes that we would only expect to see within an unconditional

434 UKCP18 PPE-type ensemble of total sample size 10,000 (for the period 2061-2080, this

435 would be 500 members * 20 years = 10,000 samples). Table 2 supports the picture that the

436 HOT2 ensemble was significantly primed towards producing extremes: the relative risk of a

437 1-in-100 year event was 10 times greater in the HOT2 ensemble than the UKCP18 PPE for

438 both hot (TXm) and wet (PRm) extremes.

439 In addition to the SST preconditioning, the dynamical situation of the study winter also made
 440 an extreme season more likely, as shown by the horizontal lines representing the likely range
 441 of the analog subsamples in Figure 4A. Based on the number of analogs sampled, the
 442 frequency of this particular large-scale flow was increased by a factor of 3.6 [2.6 , 5.4]
 443 relative to the climatological frequency estimated using the ExSamples baseline ensemble,
 444 which may be due to the prescribed boundary conditions. This would fit within the canonical
 445 picture that the negative La Nina ENSO phase is associated with positive NAO (Brönnimann,
 446 2007; Deser et al., 2017).

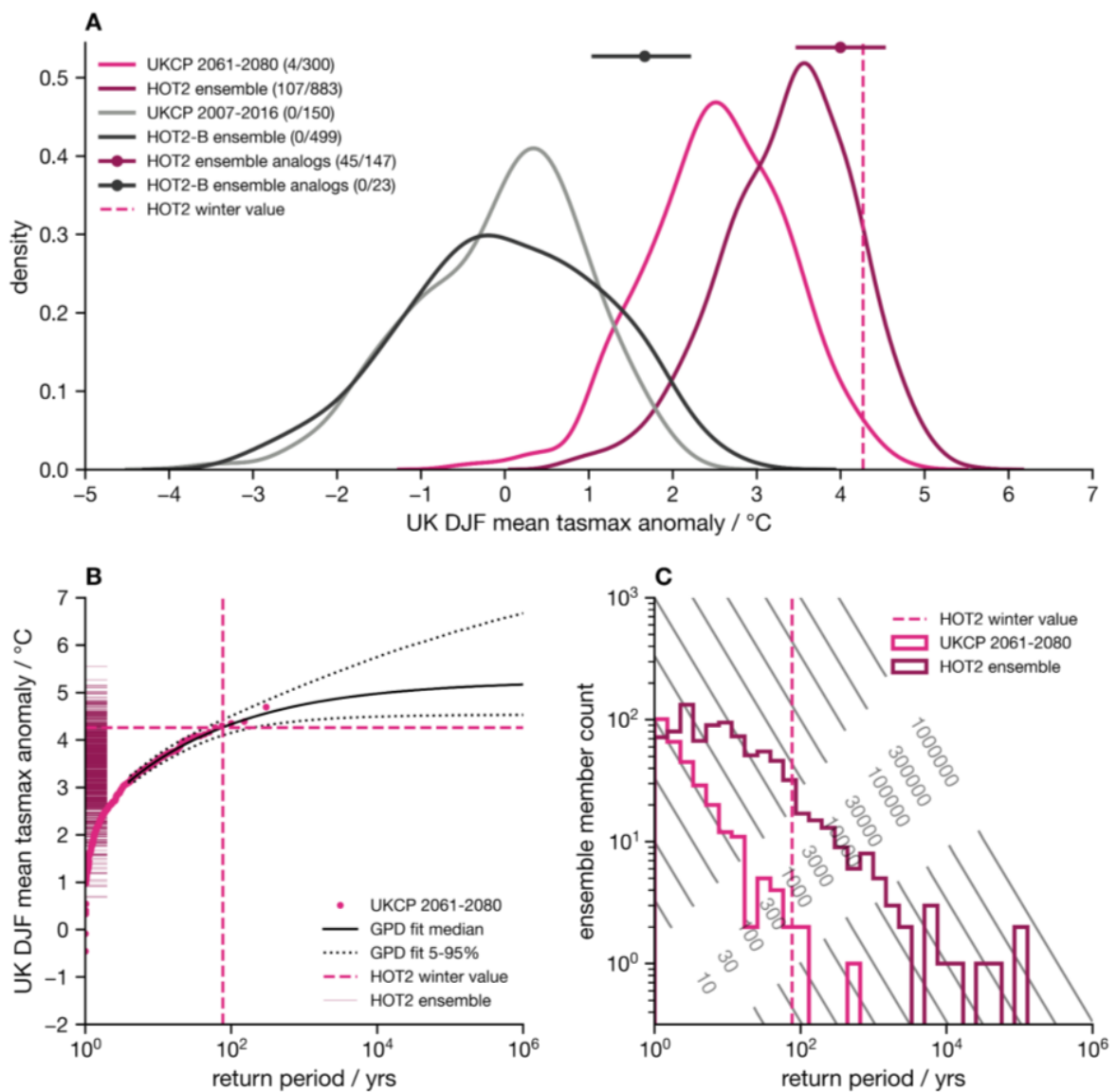


FIG 4: as FIG 4, but for the HOT2 winter.

447 3.2.3 WET

448 Finally, we examine the WET winter extreme. As in both hot winters, the magnitude of the
449 extreme within the study winter lies within the range of the WET ensemble.

450 As in the HOT2 ensemble, the prescribed SST/SIC have conditioned the WET ensemble
451 towards producing more wet extremes than would be expected from an unconditioned
452 ensemble, as shown by the histogram of sampled return periods and shifted PDF compared
453 to the UKCP 2061-2080 PDF in Figure 5. This is consistent with the quantitative estimates in
454 Table 2, which suggest that the WET ensemble was 5 times more likely to produce a 1-in-20
455 year wet (PR_m) extreme, and 12 times more likely to produce a 1-in-100 year extreme.

456 An analog-based dynamical analysis shows that, once again, the large-scale circulation
457 pattern present in the study winter was important for the development of the extreme rainfall
458 that was simulated, consistent with previous weather pattern studies (Richardson et al., 2018,
459 2020). Interestingly, conditioning on the study winter dynamics appears to have a smaller
460 influence on the WET ensemble than on the corresponding baseline: the difference between
461 the distributions implied by the PDF and by the dotted bar is much greater for the baseline
462 simulations (black) than for the future simulations (dark blue) in Figure 5A. This may be due
463 to the SST/SIC preconditioning present in the 2072 ensemble.

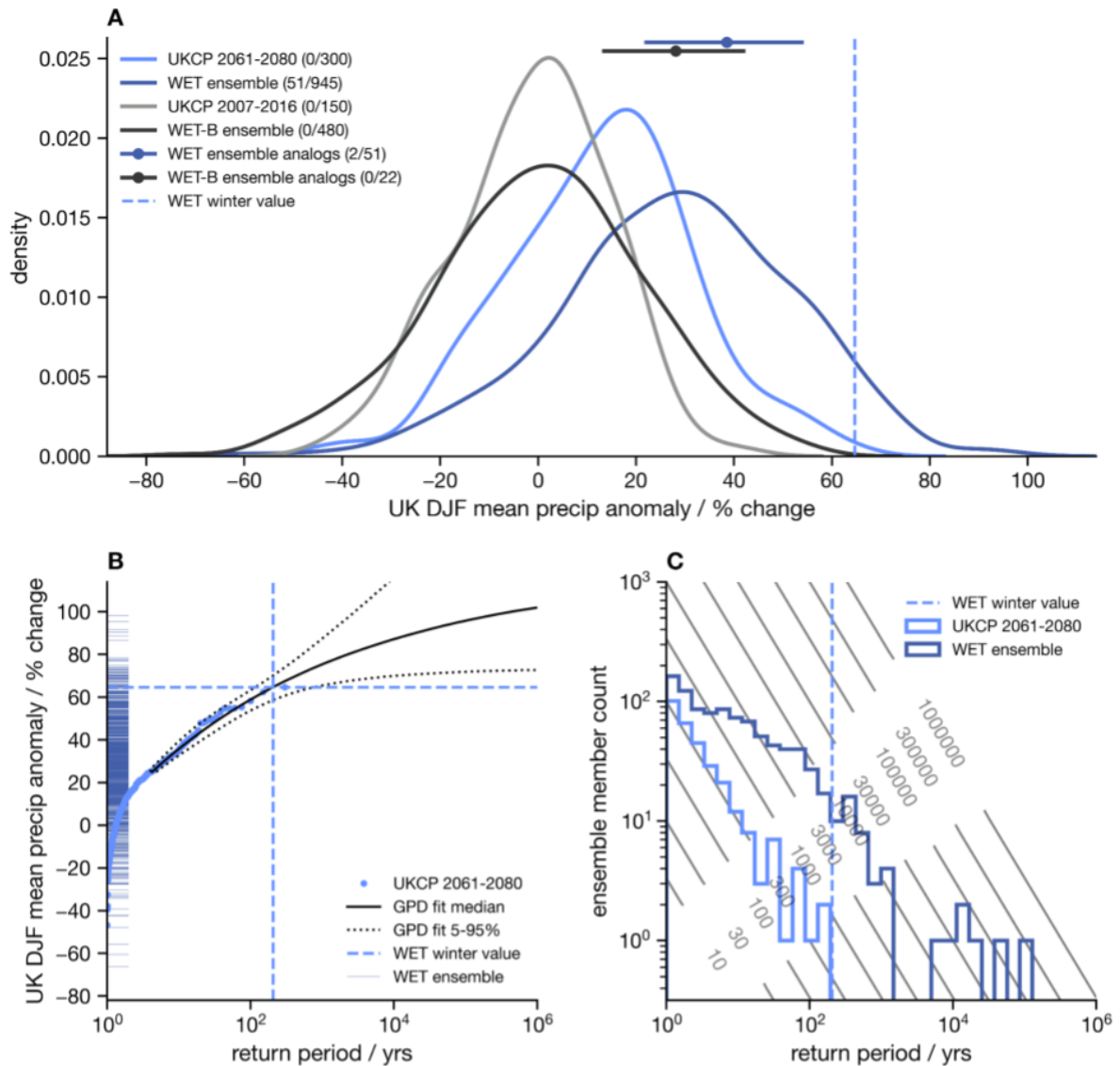


FIG 5: as FIG 4, but of DJF mean precipitation averaged over the UK region for the WET winter.

464 3.3 Sampling record-shattering subseasonal events

465 Although this study is largely concerned with extremes that occur on seasonal timescales, the

466 novel large ensembles created here also provide a set of extremes occurring on shorter

467 weather timescales. Such extreme weather events are of particular importance for decisions

468 surrounding adaptation to climate change. The “H++” scenario concept has been developed

469 to inform such adaptation decisions by considering plausible low likelihood but high impact

470 events that might test the limits to adaptation (D. King et al., 2015; Lowe et al., 2009; Wade

471 et al., 2015). Here we consider how the ExSamples methodology could be used to supplement
472 the UKCP18 PPE with regard to such H++ scenarios by examining a particular ExSamples
473 ensemble member as a case study.

474 This case study is an example of extreme DJF maximum of daily maximum temperatures
475 averaged over the UK (TXx as previously defined). Figure 6 shows a return period diagram of
476 UKCP 2061-2080 TXx deviations (centered on the mean anomaly for 2061-2071 over
477 2007-2016), plus a fitted generalised extreme value distribution (GEV) and associated
478 uncertainty. GEVs are often used to statistically model block maxima of climate variables; and
479 therefore infer information about the likelihood of such extreme events (S. J. Brown et al.,
480 2014). However, this statistical approach appears to have inadequately accounted for the risk
481 of very high impact events, an issue noted previously by Sippel et al. (2015). The dashed dark
482 orange line in Figure 6 shows the TXx for HOT1 ensemble member c0qu, which lies
483 considerably above (by 2.3 °C) any UKCP18 PPE samples. This event is roughly 5 standard
484 deviations above the mean of the UKCP18 deviations distribution shown in Figure 6. This is
485 an example of a potential “record-shattering” event as discussed by Fischer et al. (2021).
486 Since the particular GEV fitted to the UKCP18 deviations is type III (Coles, 2001), it sets a
487 theoretical upper bound on TXx, consistent with the physical laws governing energy transfer
488 in the climate system. However, in a 100,000 member resample bootstrap, the UKCP inferred
489 GEV upper bound is only above this most extreme member in 0.3 % of resamples. This is not
490 due to a mean bias between the two models: they display near-identical climatological
491 distributions of TXx over the baseline period. We note that this exceptional TXx extreme
492 arises from a very similar set of meteorological circumstances (not shown) to the
493 record-breaking winter temperature extreme that occurred over Europe in 2019 (Kendon et
494 al., 2020; Young & Galvin, 2020). Therefore, the methodology used here could help to provide
495 examples of the kinds of H++ scenarios used to consider the limits to adaptation.

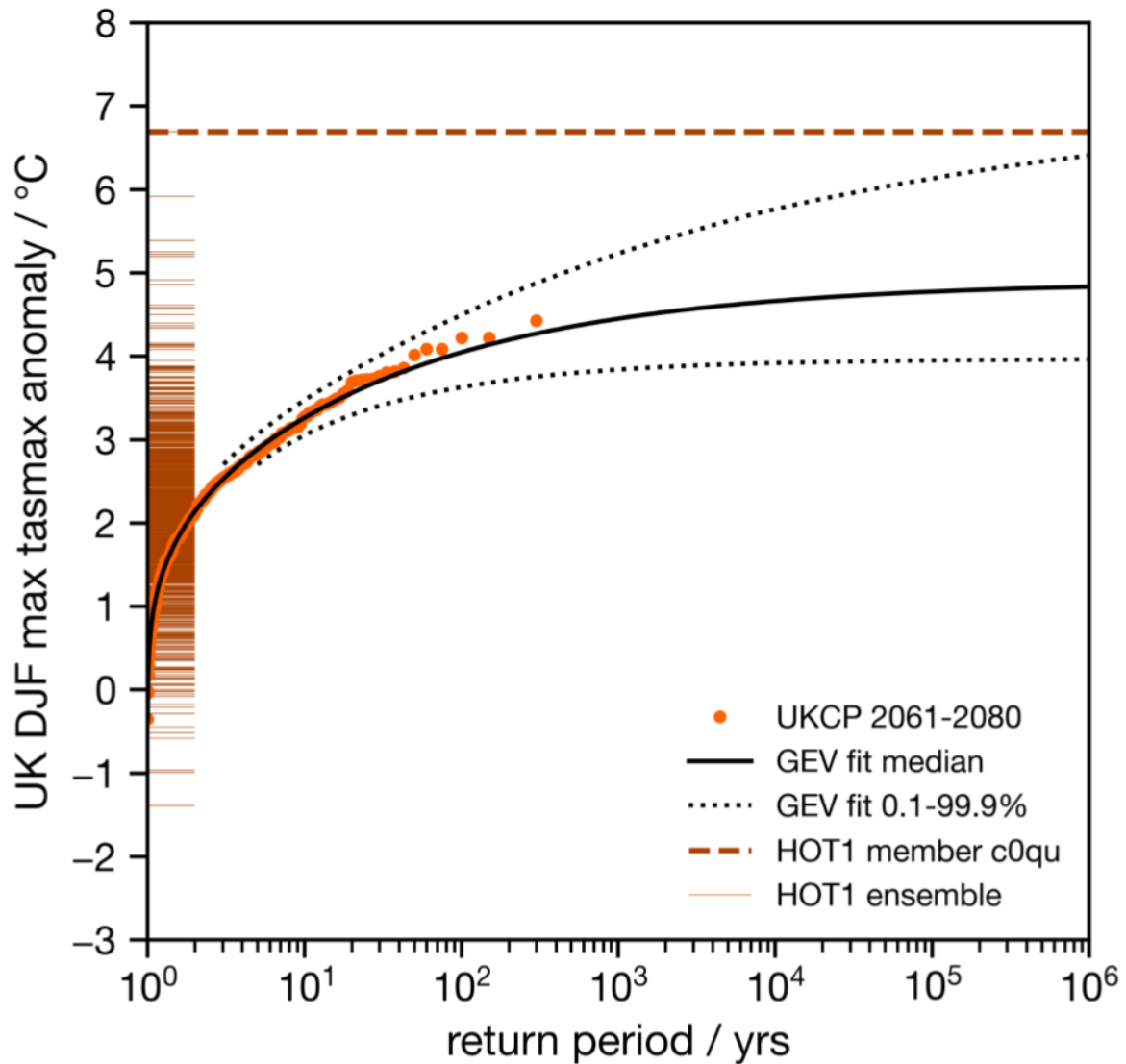


FIG 6: as return period diagram of FIG 4, but of DJF maximum of maximum daily temperatures averaged over the UK region for the HOT1 winter. The statistical model fit indicated by the solid and dotted black lines is a generalised extreme value distribution over the entire population. Note the dotted lines indicate a 0.1 - 99.9 % CI in this instance. The dashed dark orange line shows the value of the most extreme member within the HOT1 ensemble.

496 4. Discussion

497 The first science question we aimed to answer through our experiments is also the most
 498 straightforward: is the atmosphere-only HadAM4 model able to simulate the highest
 499 extremes observed in the UKCP18 HadGEM3-GC3.05 PPE, or do the differences between the
 500 models preclude HadAM4 from producing such events? The answer to this is a confident yes.

501 We have found that HadAM4 is not only able to closely reproduce the present-day climate
502 statistics of the more complex model (after correcting the bias in seasonal mean rainfall,
503 which may be due to model parameterisation), but is able to produce winters just as extreme
504 as the selected study winters when driven by the SST and SICs from those winters.

505 The question that naturally follows on from this is: were the selected winters genuinely
506 exceptional events, or could they have been more extreme? Despite the fact the selected
507 winters were already far into the tails of the projected climate distribution from UKCP18, the
508 SST/SIC forced ExSamples experiments show that higher extremes are possible. In the two
509 winters pre-conditioned by the SST and SIC patterns, there were more higher extremes than
510 in the winter where the ocean pattern did not contribute to the extreme. Since the ExSamples
511 ensembles are forced by the same lower boundary conditions as the study winters, they
512 cannot be used to determine the unconditional likelihood of these higher extremes, but they
513 do provide plausible and physically consistent scenarios in which such higher extremes
514 might be generated.

515 We suggest that the ExSamples methodology is more efficient at sampling extremes than the
516 simplest alternative approach of increasing the UKCP18 PPE size. We have found that overall,
517 for both hot and wet extremes, on both seasonal and daily timescales, the future ExSamples
518 ensembles were able to produce many more samples of extreme winters than would be
519 expected if we simply increased the UKCP18 2061-2080 ensemble to be the same size as
520 the ExSamples ensembles. Across the three future ExSamples ensembles, for mean
521 temperature we sampled 44 winters above the most extreme winter in UKCP18, and 106 for
522 mean precipitation (using re-centered deviations to define the UKCP18 maxima as shown in
523 Figures 3-5, S4-S6). However, there is an important caveat to bear in mind here: the
524 SST/SICs taken from the selected study winters clearly “primed” the corresponding
525 ExSamples ensembles towards producing relatively more extremes in two of the three cases

526 (HOT2 and WET), but not in the third (HOT1). For the two primed study winters, the benefits of
527 the ExSamples methodology is clear: we get many more samples of extreme winters than
528 would be expected from an unconditioned ensemble of the same size (like the UKCP18 PPE).
529 In particular, the HOT2 ensemble produces 10 times more samples of 1-in-100 year TXm and
530 PRm events than would be expected for an equal-size UKCP18 PPE (from Table 2). For the
531 third study winter the overall benefits to sampling efficiency are less clear. However, this
532 winter generated a TXx extreme that far exceeds anything seen in the UKCP18 PPE (and
533 indeed anything that would be expected to be seen even if the UKCP18 PPE was considerably
534 larger, based on a statistical extreme value analysis).

535 In addition to the methodology presented here, the future ExSamples ensembles explored
536 here represent a data set that may be of considerable interest to the wider scientific
537 community, since they provide multivariate spatially coherent information for climate
538 projections of very high return period extremes. These ensembles, and in particular the
539 physically plausible simulations of extremes within, could be used in the context of “H++
540 scenarios” to explore and understand the potential impacts of climate change, and the limits
541 to adaptation planning (Wade et al., 2015). The efficiency with which we have been able to
542 sample extremes with the ExSamples methodology means that we can provide a much richer
543 set of future extreme winter events than exist within the UKCP18 PPE. This rich set of events
544 could be used, for example, by impact modelling, to more fully explore the space of impacts
545 that may arise from climate change.

546 A final topic that this study touches on is the use of atmosphere-only versus coupled models.
547 Here, we have explored both present-day baseline and projected climates from a coupled
548 model (HadGEM3-GC3.05) and a comparable atmosphere-only model (HadAM4). It has
549 previously been found that atmosphere-only simulations can underestimate the internal
550 variability of the climate system (Fischer et al., 2018; He & Soden, 2016), thereby producing

551 biases in the estimated frequency of extreme events and their changes in frequency with
552 climate change, though this is an area of ongoing research (Barsugli & Battisti, 1998; Copsey
553 et al., 2006; Dong et al., 2017; Saravanan, 1998). However, for the UK region studied here, we
554 have not found that this is the case. For the baseline period, the atmosphere-only model did
555 not systematically underestimate the internal variability of the seasonal (or daily) timescale
556 extreme variables considered here (Figures 3-5, S4-S12). Since we only have ExSamples
557 future ensembles for three different sets of SST/SIC conditions, it is more difficult to quantify
558 whether the projected internal variability is significantly different from the coupled model
559 simulations, but the climate distributions of the relatively unconditioned HOT1 ensemble
560 suggest that this is not the case.

561 If the ExSamples methodology were to be repeated, for the purpose of sampling additional
562 extremes, being able to pre-select study winters (ie. lower boundary conditions) that
563 condition the resulting ensembles towards extremes would be of considerable value. Here,
564 we simply chose three of the most extreme winters within the UKCP18 PPE, expecting that
565 these would be more likely to produce extremes than a randomly selected winter. This turned
566 out to be the case for two of the winters we chose, but not the third. Understanding what
567 features of the prescribed SST and SIC patterns caused the ensembles to be conditioned
568 towards extremes would be a very useful direction for further study to take. If future research
569 were able to provide evidence of such features, then we could pre-select study winters more
570 intelligently, and therefore sample extremes even more efficiently. There has been some
571 previous work done on the subject of how SST patterns affect seasonal mid-latitude weather
572 that could potentially be used in this manner (Baker et al., 2019). On a related note, our
573 methodology could be used to understand real extremes in the present-day by driving the
574 model with observed rather than simulated SST/SICs. This would allow some exploration of
575 whether extremes that have already occurred might have been even more extreme.

576 Another research direction that could be taken would be to attempt to extract additional
577 information from the existing set of events provided by the ExSamples ensembles presented
578 here. Although the ~60 km (N216) resolution of both the ExSamples ensemble and UKCP18
579 PPE is very competitive within the context of the current generation of climate models
580 (*CMIP6 Source_id Values*, n.d.; Eyring et al., 2016), it is still relatively coarse for providing
581 assessments of weather events on small spatial or temporal scales. For example,
582 catchment-scale hydrological modelling would require much higher spatial resolutions
583 (Charlton et al., 2006). Hence, we suggest that the ExSamples ensembles could be
584 statistically downscaled (or dynamically downscaled using a regional model if suitable model
585 output was stored to drive these models) in order to provide information that is more relevant
586 for localised climate change adaptation planning. Such downscaling could result in an
587 extensive set of extreme local scenarios to complement the raw model output that provides a
588 corresponding set of extreme national scenarios. For downscaling to be trustworthy, the
589 large-scale dynamical features of the input simulations must be an accurate representation
590 of reality. The analysis that we have performed here suggests this is the case: as
591 demonstrated in the [Supplementary Information](#), the large-scale dynamics over the
592 Euro-Atlantic sector within HadAM4 very closely replicates those within HadGEM3-GC3.05.

593 **5. Concluding remarks**

594 In this study we have presented a new set of ~1000-member ensembles of simulations from
595 the HadAM4 atmosphere-only model, run on the personal computers of volunteers using a
596 distributed computing system, to allow the study of extreme weather events. The lower
597 boundary conditions of these ensembles were taken from three of the most extreme winters
598 within the UKCP18 PPE between 2061-2080, and they therefore represent a comprehensive
599 sampling of atmospheric internal variability conditioned on the prescribed SST, SIC and

600 anthropogenic forcings. Corresponding ensembles for a 2007-2016 baseline period were also
601 run to enable the HadAM4 model to be verified against the coupled HadGEM3-GC3.05
602 model used in UKCP18.

603 We find that the HadAM4 ensembles are able to simulate winters with temperature and
604 precipitation anomalies that exceed the magnitudes of the most extreme examples within
605 the UKCP18 PPE. Conditioning from the prescribed SST/SICs present in two of the three
606 ensembles resulted in significantly more extremes being sampled by these ensembles than
607 would be expected from a UKCP18 PPE-style ensemble of the same size: around 10 times
608 more 1-in-100 year extremes.

609 The computational efficiency with which our methodology was able to sample such extremes
610 provides a compelling argument for how it could be used to support future climate projection
611 efforts. The ensembles that we have presented here could themselves be used to provide
612 physically plausible simulations of extreme weather in the context of H++ scenarios and for
613 adaptation planning. Although we have focussed on the UK in this study, our methodology
614 could be applied to other regions, subject to proper model validation (Murphy et al., 2018;
615 Watson et al., 2020).

616 **Acknowledgements**

617 NJL was supported by the Natural Environment Research Council (grant no. NE/L002612/1).
618 PAGW was supported by a Natural Environmental Research Council Independent Research
619 Fellowship (grant no. NE/S014713/1).

620 We thank Myles R. Allen for his input to the initial discussions of this project, and linking the
621 members of this authorship team up. We thank Jason Lowe for his helpful comments and
622 suggestions regarding the text.

623 We thank all of the volunteers who have donated their computing time to
624 climateprediction.net to perform the HadAM4 simulations. The UK Climate Resilience
625 programme is supported by the UKRI Strategic Priorities Fund. The programme is
626 co-delivered by the Met Office and NERC on behalf of UKRI partners AHRC, EPSRC, ESRC.

627 **Code and data availability**

628 The code used to carry out the analysis and produce the figures within this study are
629 available at <https://github.com/njleach/ExSamples-analysis-notebooks>.

630 The novel ExSamples data used in this study are available from MASS via the CEDA archive
631 (<https://help.jasmin.ac.uk/category/227-mass>). They are located at
632 /adhoc/projects/qump_hadgem3/ExSamples/netcdf/product/20210622. The UKCP data used
633 in this study are available from the CEDA archive
634 (<http://data.ceda.ac.uk/badc/ukcp18/data/land-gcm/global/60km/rcp85>).

635 **References**

- 636 Allen, M. (1999). Do-it-yourself climate prediction. *Nature*, 401(6754), 642–642.
637 <https://doi.org/10.1038/44266>
- 638 Allen, M. R., Frame, D. J., Huntingford, C., Jones, C. D., Lowe, J. A., Meinshausen, M., &
639 Meinshausen, N. (2009). Warming caused by cumulative carbon emissions towards
640 the trillionth tonne. *Nature*, 458(7242), 1163–1166.
641 <https://doi.org/10.1038/nature08019>
- 642 Anderson, D. P. (2004). BOINC: A system for public-resource computing and storage. *Fifth*
643 *IEEE/ACM International Workshop on Grid Computing*, 4–10.
644 <https://doi.org/10.1109/GRID.2004.14>

645 Baker, H. S., Woollings, T., Forest, C. E., & Allen, M. R. (2019). The Linear Sensitivity of the
646 North Atlantic Oscillation and Eddy-Driven Jet to SSTs. *Journal of Climate*, 32(19),
647 6491–6511. <https://doi.org/10.1175/JCLI-D-19-0038.1>

648 Barsugli, J. J., & Battisti, D. S. (1998). The Basic Effects of Atmosphere–Ocean Thermal
649 Coupling on Midlatitude Variability. *Journal of the Atmospheric Sciences*, 55(4),
650 477–493. [https://doi.org/10.1175/1520-0469\(1998\)055<0477:TBEAO>2.0.CO;2](https://doi.org/10.1175/1520-0469(1998)055<0477:TBEAO>2.0.CO;2)

651 Bevacqua, E., Shepherd, T. G., Watson, P. A. G., Sparrow, S., Wallom, D., & Mitchell, D. (2021).
652 Larger Spatial Footprint of Wintertime Total Precipitation Extremes in a Warmer
653 Climate. *Geophysical Research Letters*, 48(8), e2020GL091990.
654 <https://doi.org/10.1029/2020GL091990>

655 Brönnimann, S. (2007). Impact of El Niño–Southern Oscillation on European climate. *Reviews*
656 *of Geophysics*, 45(3). <https://doi.org/10.1029/2006RG000199>

657 Brown, A., Milton, S., Cullen, M., Golding, B., Mitchell, J., & Shelly, A. (2012). Unified Modeling
658 and Prediction of Weather and Climate: A 25-Year Journey. *Bulletin of the American*
659 *Meteorological Society*, 93(12), 1865–1877.
660 <https://doi.org/10.1175/BAMS-D-12-00018.1>

661 Brown, S. J., Murphy, J. M., Sexton, D. M. H., & Harris, G. R. (2014). Climate projections of
662 future extreme events accounting for modelling uncertainties and historical
663 simulation biases. *Climate Dynamics*, 43(9), 2681–2705.
664 <https://doi.org/10.1007/s00382-014-2080-1>

665 Cattiaux, J., Vautard, R., Cassou, C., Yiou, P., Masson-Delmotte, V., & Codron, F. (2010). Winter
666 2010 in Europe: A cold extreme in a warming climate. *Geophysical Research Letters*,
667 37(20). <https://doi.org/10.1029/2010GL044613>

668 Charlton, R., Fealy, R., Moore, S., Sweeney, J., & Murphy, C. (2006). Assessing the Impact of
669 Climate Change on Water Supply and Flood Hazard in Ireland Using Statistical
670 Downscaling and Hydrological Modelling Techniques. *Climatic Change*, 74(4),

671 475–491. <https://doi.org/10.1007/s10584-006-0472-x>

672 *CMIP6 source_id values*. (n.d.). Retrieved 10 August 2021, from

673 https://wcrp-cmip.github.io/CMIP6_CVs/docs/CMIP6_source_id.html

674 Coles, S. (2001). *An Introduction to Statistical Modeling of Extreme Values*. Springer-Verlag.

675 <https://doi.org/10.1007/978-1-4471-3675-0>

676 Copesey, D., Sutton, R., & Knight, J. R. (2006). Recent trends in sea level pressure in the Indian

677 Ocean region. *Geophysical Research Letters*, 33(19).

678 <https://doi.org/10.1029/2006GL027175>

679 Deser, C., Alexander, M. A., Xie, S.-P., & Phillips, A. S. (2010). Sea Surface Temperature

680 Variability: Patterns and Mechanisms. *Annual Review of Marine Science*, 2(1), 115–143.

681 <https://doi.org/10.1146/annurev-marine-120408-151453>

682 Deser, C., Simpson, I. R., McKinnon, K. A., & Phillips, A. S. (2017). The Northern Hemisphere

683 Extratropical Atmospheric Circulation Response to ENSO: How Well Do We Know It

684 and How Do We Evaluate Models Accordingly? *Journal of Climate*, 30(13),

685 5059–5082. <https://doi.org/10.1175/JCLI-D-16-0844.1>

686 Diffenbaugh, N. S., Singh, D., Mankin, J. S., Horton, D. E., Swain, D. L., Touma, D., Charland, A.,

687 Liu, Y., Haugen, M., Tsiang, M., & Rajaratnam, B. (2017). Quantifying the influence of

688 global warming on unprecedented extreme climate events. *Proceedings of the*

689 *National Academy of Sciences*, 114(19), 4881–4886.

690 <https://doi.org/10.1073/pnas.1618082114>

691 Dong, B., Sutton, R. T., Shaffrey, L., & Klingaman, N. P. (2017). Attribution of Forced Decadal

692 Climate Change in Coupled and Uncoupled Ocean–Atmosphere Model Experiments.

693 *Journal of Climate*, 30(16), 6203–6223. <https://doi.org/10.1175/JCLI-D-16-0578.1>

694 Eyring, V., Bony, S., Meehl, G. A., Senior, C. A., Stevens, B., Stouffer, R. J., & Taylor, K. E. (2016).

695 Overview of the Coupled Model Intercomparison Project Phase 6 (CMIP6)

696 experimental design and organization. *Geoscientific Model Development*, 9(5),

697 1937–1958. <https://doi.org/10.5194/gmd-9-1937-2016>

698 Fischer, E. M., Beyerle, U., Schleussner, C. F., King, A. D., & Knutti, R. (2018). Biased Estimates
699 of Changes in Climate Extremes From Prescribed SST Simulations. *Geophysical*
700 *Research Letters*, 45(16), 8500–8509. <https://doi.org/10.1029/2018GL079176>

701 Fischer, E. M., Sippel, S., & Knutti, R. (2021). Increasing probability of record-shattering
702 climate extremes. *Nature Climate Change*, 1–7.
703 <https://doi.org/10.1038/s41558-021-01092-9>

704 Frame, D. J., Aina, T., Christensen, C. M., Faull, N. E., Knight, S. H. E., Piani, C., Rosier, S. M.,
705 Yamazaki, K., Yamazaki, Y., & Allen, M. R. (2009). The climateprediction.net BBC
706 climate change experiment: Design of the coupled model ensemble. *Philosophical*
707 *Transactions of the Royal Society A: Mathematical, Physical and Engineering*
708 *Sciences*, 367(1890), 855–870. <https://doi.org/10.1098/rsta.2008.0240>

709 Francis, J. A., & Vavrus, S. J. (2012). Evidence linking Arctic amplification to extreme weather
710 in mid-latitudes. *Geophysical Research Letters*, 39(6).
711 <https://doi.org/10.1029/2012GL051000>

712 Gessner, C., Fischer, E. M., Beyerle, U., & Knutti, R. (2021). Very Rare Heat Extremes:
713 Quantifying and Understanding Using Ensemble Reinitialization. *Journal of Climate*,
714 34(16), 6619–6634. <https://doi.org/10.1175/JCLI-D-20-0916.1>

715 He, J., & Soden, B. J. (2016). Does the Lack of Coupling in SST-Forced Atmosphere-Only
716 Models Limit Their Usefulness for Climate Change Studies? *Journal of Climate*,
717 29(12), 4317–4325. <https://doi.org/10.1175/JCLI-D-14-00597.1>

718 Hodges, J. L. (1958). The significance probability of the smirnov two-sample test. *Arkiv För*
719 *Matematik*, 3(5), 469–486. <https://doi.org/10.1007/BF02589501>

720 Hosking, J. R. M. (1990). L-Moments: Analysis and Estimation of Distributions Using Linear
721 Combinations of Order Statistics. *Journal of the Royal Statistical Society: Series B*
722 *(Methodological)*, 52(1), 105–124. <https://doi.org/10.1111/j.2517-6161.1990.tb01775.x>

723 Hosking, J. R. M., & Wallis, J. R. (1987). Parameter and Quantile Estimation for the Generalized
724 Pareto Distribution. *Technometrics*, 29(3), 339–349.
725 <https://doi.org/10.1080/00401706.1987.10488243>

726 Hosking, J. R. M., & Wallis, J. R. (1997). Regional Frequency Analysis. In *Regional Frequency*
727 *Analysis*. Cambridge University Press. <https://doi.org/10.1017/cbo9780511529443>

728 Hosking, J. R. M., Wallis, J. R., & Wood, E. F. (1985). Estimation of the generalized
729 extreme-value distribution by the method of probability-weighted moments.
730 *Technometrics*, 27(3), 251–261. <https://doi.org/10.1080/00401706.1985.10488049>

731 Huang, W. T. K., Charlton-Perez, A., Lee, R. W., Neal, R., Sarran, C., & Sun, T. (2020). Weather
732 regimes and patterns associated with temperature-related excess mortality in the UK:
733 A pathway to sub-seasonal risk forecasting. *Environmental Research Letters*, 15(12),
734 124052. <https://doi.org/10.1088/1748-9326/abcbb>

735 Karmalkar, A. V., Sexton, D. M. H., Murphy, J. M., Booth, B. B. B., Rostron, J. W., & McNeall, D. J.
736 (2019). Finding plausible and diverse variants of a climate model. Part II:
737 Development and validation of methodology. *Climate Dynamics*, 53(1), 847–877.
738 <https://doi.org/10.1007/s00382-019-04617-3>

739 Kendon, M., Sexton, D., & McCarthy, M. (2020). A temperature of 20°C in the UK winter: A
740 sign of the future? *Weather*, 75(10), 318–324. <https://doi.org/10.1002/wea.3811>

741 King, D., Schrag, D., Dadi, Z., Ye, Q., & Ghosh, A. (2015). *Climate change: A risk assessment*.
742 UK Foreign & Commonwealth Office.
743 <https://www.csap.cam.ac.uk/projects/climate-change-risk-assessment/>

744 King, M. P., Herceg-Bulić, I., Bladé, I., García-Serrano, J., Keenlyside, N., Kucharski, F., Li, C., &
745 Sobolowski, S. (2018). Importance of Late Fall ENSO Teleconnection in the
746 Euro-Atlantic Sector. *Bulletin of the American Meteorological Society*, 99(7),
747 1337–1343. <https://doi.org/10.1175/BAMS-D-17-0020.1>

748 King, M. P., Yu, E., & Sillmann, J. (2020). Impact of strong and extreme El Niños on European

749 hydroclimate. *Tellus A: Dynamic Meteorology and Oceanography*, 72(1), 1–10.
750 <https://doi.org/10.1080/16000870.2019.1704342>

751 Kolmogorov, A. N. (1933). Sulla Determinazione Empirica di Una Legge di Distribuzione.
752 *Giornale Dell'Istituto Italiano Degli Attuari*, 4, 83–91.

753 Kretschmer, M., Zappa, G., & Shepherd, T. G. (2020). The role of Barents–Kara sea ice loss in
754 projected polar vortex changes. *Weather and Climate Dynamics*, 1(2), 715–730.
755 <https://doi.org/10.5194/wcd-1-715-2020>

756 Kysely, J., & Picek, J. (2007). Probability estimates of heavy precipitation events in a
757 flood-prone central-European region with enhanced influence of Mediterranean
758 cyclones. *Advances in Geosciences*, 12, 43–50.
759 <https://doi.org/10.5194/adgeo-12-43-2007>

760 López-Parages, J., Rodríguez-Fonseca, B., Dommenges, D., & Frauen, C. (2016). ENSO
761 influence on the North Atlantic European climate: A non-linear and non-stationary
762 approach. *Climate Dynamics*, 47(7), 2071–2084.
763 <https://doi.org/10.1007/s00382-015-2951-0>

764 Lowe, J. A., Bernie, D., Bett, P., Bricheno, L., Brown, S., Calvert, D., Clark, R., Eagle, K., Edwards,
765 T., Fosser, G., Fung, F., Gohar, L., Good, P., Gregory, J., Harris, G., Howard, T., Kaye, N.,
766 Kendon, E., Krijnen, J., ... Belcher, S. (2018). *UKCP18 Science Overview Report*. Met
767 Office Hadley Centre.
768 [https://www.metoffice.gov.uk/pub/data/weather/uk/ukcp18/science-reports/UKCP18-O](https://www.metoffice.gov.uk/pub/data/weather/uk/ukcp18/science-reports/UKCP18-Overview-report.pdf)
769 [verview-report.pdf](https://www.metoffice.gov.uk/pub/data/weather/uk/ukcp18/science-reports/UKCP18-Overview-report.pdf)

770 Lowe, J. A., Howard, T. P., Pardaens, A., Tinker, J., Holt, J., Wakelin, S., Milne, G., Leake, J., Wolf,
771 J., Horsburgh, K., Reeder, T., Jenkins, G., Ridley, J., Dye, S., & Bradley, S. (2009). *UK*
772 *Climate Projections science report: Marine and coastal projections*. Met Office Hadley
773 Centre.
774 https://webarchive.nationalarchives.gov.uk/ukgwa/20181204111026mp_/http://ukclimat

775 eprojections-ukcp09.metoffice.gov.uk/media.jsp?mediaid=87906&filetype=pdf

776 Marani, M., & Ignaccolo, M. (2015). A metastatistical approach to rainfall extremes. *Advances*
777 *in Water Resources*, 79, 121–126. <https://doi.org/10.1016/j.adwatres.2015.03.001>

778 Murphy, J. M., Harris, G. R., Sexton, D. M. H., Kendon, E. J., Bett, P. E., Clark, R. T., Eagle, K. E.,
779 Fosser, G., Fung, F., Lowe, J. A., McDonald, R. E., McInnes, R. N., McSweeney, C. F.,
780 Mitchell, J. F. B., Rostron, J. W., Thornton, H. E., Tucker, S., & Yamazaki, K. (2018).
781 *UKCP18 Land Projections: Science Report*. Met Office.
782 <https://www.metoffice.gov.uk/pub/data/weather/uk/ukcp18/science-reports/UKCP18-L>
783 [and-report.pdf](https://www.metoffice.gov.uk/pub/data/weather/uk/ukcp18/science-reports/UKCP18-L)

784 Neal, R., Fereday, D., Crocker, R., & Comer, R. E. (2016). A flexible approach to defining
785 weather patterns and their application in weather forecasting over Europe.
786 *Meteorological Applications*, 23(3), 389–400. <https://doi.org/10.1002/met.1563>

787 Pall, P., Aina, T., Stone, D. A., Stott, P. A., Nozawa, T., Hilberts, A. G. J., Lohmann, D., & Allen, M.
788 R. (2011). Anthropogenic greenhouse gas contribution to flood risk in England and
789 Wales in autumn 2000. *Nature*, 470(7334), 382–385.
790 <https://doi.org/10.1038/nature09762>

791 Pedersen, R. A., Cvijanovic, I., Langen, P. L., & Vinther, B. M. (2016). The Impact of Regional
792 Arctic Sea Ice Loss on Atmospheric Circulation and the NAO. *Journal of Climate*,
793 29(2), 889–902. <https://doi.org/10.1175/JCLI-D-15-0315.1>

794 Pope, V. D., Gallani, M. L., Rowntree, P. R., & Stratton, R. A. (2000). The impact of new physical
795 parametrizations in the Hadley Centre climate model: HadAM3. *Climate Dynamics*,
796 16(2), 123–146. <https://doi.org/10.1007/s003820050009>

797 Rahmstorf, S., & Coumou, D. (2011). Increase of extreme events in a warming world.
798 *Proceedings of the National Academy of Sciences of the United States of America*,
799 108(44), 17905–17909. <https://doi.org/10.1073/pnas.1101766108>

800 Riahi, K., Rao, S., Krey, V., Cho, C., Chirkov, V., Fischer, G., Kindermann, G., Nakicenovic, N., &

801 Rafaj, P. (2011). RCP 8.5—A scenario of comparatively high greenhouse gas
802 emissions. *Climatic Change*, 109(1-2), 33–57.
803 <https://doi.org/10.1007/s10584-011-0149-y>

804 Richardson, D., Fowler, H. J., Kilsby, C. G., & Neal, R. (2018). A new precipitation and drought
805 climatology based on weather patterns. *International Journal of Climatology*, 38(2),
806 630–648. <https://doi.org/10.1002/joc.5199>

807 Richardson, D., Neal, R., Dankers, R., Mylne, K., Cowling, R., Clements, H., & Millard, J. (2020).
808 Linking weather patterns to regional extreme precipitation for highlighting potential
809 flood events in medium- to long-range forecasts. *Meteorological Applications*, 27(4),
810 e1931. <https://doi.org/10.1002/met.1931>

811 Saravanan, R. (1998). Atmospheric Low-Frequency Variability and Its Relationship to
812 Midlatitude SST Variability: Studies Using the NCAR Climate System Model. *Journal*
813 *of Climate*, 11(6), 1386–1404.
814 [https://doi.org/10.1175/1520-0442\(1998\)011<1386:ALFVAI>2.0.CO;2](https://doi.org/10.1175/1520-0442(1998)011<1386:ALFVAI>2.0.CO;2)

815 Screen, J. A. (2017). The missing Northern European winter cooling response to Arctic sea ice
816 loss. *Nature Communications*, 8(1), 14603. <https://doi.org/10.1038/ncomms14603>

817 Screen, J. A., & Simmonds, I. (2013). Exploring links between Arctic amplification and
818 mid-latitude weather. *Geophysical Research Letters*, 40(5), 959–964.
819 <https://doi.org/10.1002/grl.50174>

820 Seneviratne, S. I., Zhang, X., Adnan, M., Badi, W., Dereczynski, C., Di Luca, A., Ghosh, S.,
821 Iskandar, I., Kossin, J., Lewis, S., Otto, F., Pinto, I., Satoh, M., Vicente-Serrano, S. M.,
822 Wehner, M., & Zhou, B. (2021). Weather and Climate Extreme Events in a Changing
823 Climate. In V. Masson-Delmotte, P. Zhai, A. Pirani, S. L. Connors, C. Péan, S. Berger, N.
824 Caud, Y. Chen, L. Goldfarb, M. I. Gomis, M. Huang, K. Leitzell, E. Lonnoy, J. B. R.
825 Matthews, T. K. Maycock, T. Waterfield, O. Yelekçi, R. Yu, & B. Zhou (Eds.), *Climate*
826 *Change 2021: The Physical Science Basis. Contribution of Working Group I to the*

827 *Sixth Assessment Report of the Intergovernmental Panel on Climate Change.*
828 Cambridge University Press.
829 https://www.ipcc.ch/report/ar6/wg1/downloads/report/IPCC_AR6_WGI_Chapter_12.pdf

830 Sexton, D. M. H., Karmalkar, A. V., Murphy, J. M., Williams, K. D., Boutle, I. A., Morcrette, C. J.,
831 Stirling, A. J., & Vosper, S. B. (2019). Finding plausible and diverse variants of a
832 climate model. Part 1: Establishing the relationship between errors at weather and
833 climate time scales. *Climate Dynamics*, 53(1), 989–1022.
834 <https://doi.org/10.1007/s00382-019-04625-3>

835 Sexton, D. M. H., McSweeney, C. F., Rostron, J. W., Yamazaki, K., Booth, B. B. B., Murphy, J. M.,
836 Regayre, L., Johnson, J. S., & Karmalkar, A. V. (2021). A perturbed parameter ensemble
837 of HadGEM3-GC3.05 coupled model projections: Part 1: selecting the parameter
838 combinations. *Climate Dynamics*, 56(11), 3395–3436.
839 <https://doi.org/10.1007/s00382-021-05709-9>

840 Sexton, D. M. H., Rowell, D. P., Folland, C. K., & Karoly, D. J. (2001). Detection of
841 anthropogenic climate change using an atmospheric GCM. *Climate Dynamics*, 17(9),
842 669–685. <https://doi.org/10.1007/s003820000141>

843 Sexton, D., Yamazaki, K., Murphy, J., & Rostron, J. (2020). *Assessment of drifts and internal*
844 *variability in UKCP projections* (p. 20). Met Office.
845 [https://www.metoffice.gov.uk/binaries/content/assets/metofficegovuk/pdf/research/uk](https://www.metoffice.gov.uk/binaries/content/assets/metofficegovuk/pdf/research/ukcp/ukcp-climate-drifts-report.pdf)
846 [cp/ukcp-climate-drifts-report.pdf](https://www.metoffice.gov.uk/binaries/content/assets/metofficegovuk/pdf/research/ukcp/ukcp-climate-drifts-report.pdf)

847 Sippel, S., Mitchell, D., Black, M. T., Dittus, A. J., Harrington, L., Schaller, N., & Otto, F. E. L.
848 (2015). Combining large model ensembles with extreme value statistics to improve
849 attribution statements of rare events. *Weather and Climate Extremes*, 9, 25–35.
850 <https://doi.org/10.1016/j.wace.2015.06.004>

851 Smirnov, N. (1939a). On the estimation of the discrepancy between empirical curves of
852 distribution for two independent samples. *Bulletin Mathématique de L'Université de*

853 Moscow, 2(2), 3–11.

854 Smirnov, N. (1939b). Sur les écarts de la courbe de distribution empirique. *Matematicheskii*
855 *Sbornik*, 6(48)(1), 3–26.

856 Sparrow, S., Sexton, D., Leach, N. J., Watson, P. A. G., & Wallom, D. C. H. (2021). ExSamples
857 Simulation Dataset. *Scientific Data*, *in prep.*

858 Stainforth, D. A., Aina, T., Christensen, C., Collins, M., Faull, N., Frame, D. J., Kettleborough, J.
859 A., Knight, S., Martin, A., Murphy, J. M., Piani, C., Sexton, D., Smith, L. A., Spicer, R. A.,
860 Thorpe, A. J., & Allen, M. R. (2005). Uncertainty in predictions of the climate response
861 to rising levels of greenhouse gases. *Nature*, 433(7024), 403–406.
862 <https://doi.org/10.1038/nature03301>

863 Stainforth, D., Kettleborough, J., Allen, M., Collins, M., Heaps, A., & Murphy, J. (2002).
864 Distributed computing for public-interest climate modeling research. *Computing in*
865 *Science Engineering*, 4(3), 82–89. <https://doi.org/10.1109/5992.998644>

866 Stone, D. A., & Allen, M. R. (2005). The end-to-end attribution problem: From emissions to
867 impacts. *Climatic Change*, 71(3), 303–318.
868 <https://doi.org/10.1007/s10584-005-6778-2>

869 Stott, P. A., Stone, D. A., & Allen, M. R. (2004). Human contribution to the European heatwave
870 of 2003. *Nature*, 432(7017), 610–614. <https://doi.org/10.1038/nature03089>

871 *The Global Risks Report 2021*. (2021). World Economic Forum.
872 <https://www.weforum.org/reports/the-global-risks-report-2021/>

873 Vautard, R., Yiou, P., Otto, F., Stott, P., Christidis, N., van Oldenborgh, G. J., & Schaller, N.
874 (2016). Attribution of human-induced dynamical and thermodynamical contributions
875 in extreme weather events. *Environmental Research Letters*, 11(11), 114009.
876 <https://doi.org/10.1088/1748-9326/11/11/114009>

877 Wade, S., Sanderson, M., Golding, N., Lowe, J. A., Betts, R. A., Reynard, N., Kay, A. L., Stewart, L.,
878 Prudhomme, C., Shaffrey, L., Lloyd-Hughes, B., & Harvey, B. (2015). *Developing H++*

879 *climate change scenarios for heat waves, droughts, floods, windstorms and cold*
880 *snaps* (p. 144). Committee on Climate Change.
881 <https://www.theccc.org.uk/publication/met-office-for-the-asc-developing-h-climate-ch>
882 [ange-scenarios/](https://www.theccc.org.uk/publication/met-office-for-the-asc-developing-h-climate-ch)

883 Wan Zin, W. Z., Jemain, A. A., & Ibrahim, K. (2009). The best fitting distribution of annual
884 maximum rainfall in Peninsular Malaysia based on methods of L-moment and
885 LQ-moment. *Theoretical and Applied Climatology*, 96(3), 337–344.
886 <https://doi.org/10.1007/s00704-008-0044-2>

887 Watson, P., Sparrow, S., Ingram, W., Wilson, S., Marie, D., Zappa, G., Jones, R., Mitchell, D.,
888 Woollings, T., & Allen, M. (2020). *Multi-thousand member ensemble atmospheric*
889 *simulations with global 60km resolution using climateprediction.net* (No.
890 EGU2020-10895). EGU2020. Copernicus Meetings.
891 <https://doi.org/10.5194/egusphere-egu2020-10895>

892 Webb, M., Senior, C., Bony, S., & Morcrette, J.-J. (2001). Combining ERBE and ISCCP data to
893 assess clouds in the Hadley Centre, ECMWF and LMD atmospheric climate models.
894 *Climate Dynamics*, 17(12), 905–922. <https://doi.org/10.1007/s003820100157>

895 Williams, K. D., Copsey, D., Blockley, E. W., Bodas-Salcedo, A., Calvert, D., Comer, R., Davis, P.,
896 Graham, T., Hewitt, H. T., Hill, R., Hyder, P., Ineson, S., Johns, T. C., Keen, A. B., Lee, R.
897 W., Megann, A., Milton, S. F., Rae, J. G. L., Roberts, M. J., ... Xavier, P. K. (2018). The Met
898 Office Global Coupled Model 3.0 and 3.1 (GC3.0 and GC3.1) Configurations. *Journal*
899 *of Advances in Modeling Earth Systems*, 10(2), 357–380.
900 <https://doi.org/10.1002/2017MS001115>

901 Williams, K. D., Ringer, M. A., & Senior, C. A. (2003). Evaluating the cloud response to climate
902 change and current climate variability. *Climate Dynamics*, 20(7), 705–721.
903 <https://doi.org/10.1007/s00382-002-0303-3>

904 Yamazaki, K., Sexton, D. M. H., Rostron, J. W., McSweeney, C. F., Murphy, J. M., & Harris, G. R.

905 (2021). A perturbed parameter ensemble of HadGEM3-GC3.05 coupled model
906 projections: Part 2: global performance and future changes. *Climate Dynamics*, 56(11),
907 3437–3471. <https://doi.org/10.1007/s00382-020-05608-5>

908 Yiou, P., Jézéquel, A., Naveau, P., Otto, F. E. L., Vautard, R., & Vrac, M. (2017). A statistical
909 framework for conditional extreme event attribution. *Advances in Statistical*
910 *Climatology, Meteorology and Oceanography*, 3(1), 17–31.
911 <https://doi.org/10.5194/ascmo-3-17-2017>

912 Young, M., & Galvin, J. (2020). The record-breaking warm spell of February 2019 in Britain,
913 the Channel Islands, France and the Netherlands. *Weather*, 75(2), 36–45.
914 <https://doi.org/10.1002/wea.3664>